

## Article

# Estimation of Forest Biomass and Carbon Storage in China Based on Forest Resources Inventory Data

Jing Lu, Zhongke Feng \* and Yan Zhu

Precision Forestry Key Laboratory of Beijing, Beijing Forestry University, Beijing 10083, China

\* Correspondence: zhongkefeng@bjfu.edu.cn; Tel.: +86-138-1030-5579

Received: 24 April 2019; Accepted: 30 July 2019; Published: 1 August 2019



**Abstract:** Forests are important in the global carbon cycle and it is necessary to quickly and accurately measure forest volume to estimate forest aboveground biomass (AGB) and aboveground carbon storage (AGC). In this paper, we used data from the eighth forest resources inventory of China to establish two stand volume models based on stand density and forest basal area for 37 arbor forest types (dominant species); and performed a comparative analysis to obtain the best model. Then the AGB, AGB density, AGC, and AGC density of the different forest types and regions were estimated by conversion function methods. The results showed that: (1) The volume model of tree height and forest basal area could better fit the natural growth process of forests, and 36 of the 37 forest types had  $R^2$  greater than 0.8; (2) The average AGB density of arbor forest in China was  $95.03 \text{ Mg ha}^{-1}$  and the average AGC density was  $48.15 \text{ Mg ha}^{-1}$  (3) Among forest types, *Picea asperata* Mast., *Quercus* spp., and *Populus* spp. had the highest AGB and AGC, while *Cinnamomum camphora* (L.) Presl, *Pinus taiwanensis* Hayata, and *Pinus densiflora* Sieb. et Zucc. had the lowest. The AGB density and AGC density of *Phoebe zhennan* S. Lee et F. N. Wei and *Pinus densata* Mast. were the highest, while those of *Pinus densiflora* Sieb. et Zucc., *Pinus elliottii* Engelman, and *Eucalyptus robusta* Smith were the lowest. (4) Among regions, AGB and AGC ranging from high to low, were as follows: northwest, southwest, northeast, central south, east, and north. The northwest and southwest regions accounted for more than 70% of the country's AGB and AGC. The average AGB density and AGC density among the regions were  $91.34 \text{ Mg ha}^{-1}$  and  $46.4 \text{ Mg ha}^{-1}$ , respectively. Ranging from high to low as follows: southwest, northwest, northeast, east, central south, and north. The methods used in this paper provide a basis for fast and accurate estimation of stand volume, and the estimates of AGB and AGC have important reference value for explaining the role of ecosystems in coping with global climate change in China.

**Keywords:** stand volume; AGC; AGB; forest type; region; AGC density

## 1. Introduction

Forest ecosystems are the main component of terrestrial ecosystems. On land, although forest area accounts for only 40% of the global non-ice surface, its biomass accounts for 90% of the terrestrial biomass, and its soil carbon storage accounts for 73% of the global soil carbon storage [1,2]. In the face of global climate change, forest aboveground biomass (AGB) and aboveground carbon storage (AGC) which are the bases for studying the structure and function of forest ecosystems, have attracted wide attention worldwide [3]. At present, there are many methods for calculating AGB and AGC, among which the model based on stand volume is widely used. Stand volume is an important index for forest resources monitoring and an important basis for forestry management decision-making [4,5]. The growth and development of forests under various specific management conditions can be estimated by stand volume, and for this reason, it has been widely used in forest management, resources archives updating, forest asset assessment, and forest carbon sequestration estimation [6]. Using scientific

methods to establish stand volume models and estimate AGB and AGC can provide a basis for forest management and forest planning. However, because the current forest resources survey system in China cannot produce accurate and reliable estimates of annual forest stock, and it is meaningful to establish accurate volume models. At present, the volume of trees at the single-tree scale is usually derived from the national unary volume model related to diameter of breast height (DBH) and the national binary volume model related to DBH and tree height [7,8]. For a given stand, it is time-consuming and laborious to calculate the volume of individual timber, which is unrealistic at a large regional scale. Except for DBH and tree height, stand density is also an indispensable factors for forest growth, and the forest basal area is calculated by stand density and DBH [9]. Both of these factors can be introduced to the model to improve the accuracy of stand volume estimates.

Forest AGB and AGC distribution patterns are influenced by forest type, topography, and stand characteristics [10–14]. The estimation of forest AGB and AGC can be traced back to the 1970s in foreign countries, but it started late in China, at the beginning of the 21st century [15,16]. The conversion relationship between forest AGB and stand volume is a key link in estimating forest AGC at the national or regional scale. Forest AGB can be estimated by direct measurement and indirect methods [17]. Direct measurement involves harvesting, which has the highest accuracy, but is destructive to the ecosystem and time-consuming. Indirect methods involve AGB models (including relative growth relationship and AGB-accumulation models), AGB estimation parameters, and 3S technology [18–22]. Due to China's strict control on annual forest harvesting, the biomass-volume model has been widely used in large-scale forest AGB estimation [23]. Volume-derived AGB is generally used to estimate AGC [24,25], and 0.5 is commonly used as the conversion coefficient of AGB and AGC worldwide [26]. As the structure of forest resources in China has been changing, research employing the volume-AGB-AGC model has faced some challenges [27]. First, inaccurate estimation of AGB and AGC is directly caused by the low accuracy of stand volume acquisition. Second, many studies have involved single tree species and single tree models in small areas, but few have included large-scale stand accumulation models [28,29]. Moreover, the amount of sample plot data used for analysis is insufficient, and there is a lack of fixed sample plot data [30]. In this case, the establishment of a high-precision, large-scale stand volume model can show a great potential of applicability in forest carbon sink and ecology.

In this paper, we used fixed sample plot data from the eighth national forest resources inventory (2009–2013) to establish two models to estimate stand volume, so that under the condition of known stand factors, the stand volume can be obtained more accurately and quickly, which will in turn support the estimation of AGB and AGC. Based on the estimated forest stock, the AGB and AGC of each forest type were estimated, and the AGB density and AGC density of different forest types and regions were compared, which could lay a theoretical foundation for future forest management and planning management. This method uses a large amount of fixed sample plot data to estimate forest stock at the national and stand scales, accurately and quantitatively manages China's forest resources, and enables improved economic benefits of forest resource while encouraging sustainable development.

## 2. Materials and Methods

### 2.1. Data Collection

The national survey and inventory of forest resources refers to the survey and verification of the distribution and quality of each type of forest resources in specific regions over specific periods [31]. The essence of the national forest resources inventory in China is to reset and measure the sample plots laid out by state and local governments, which requires the accurate measurement of tree height and DBH. At the time of investigation, the GPS coordinate error should not exceed 10–15 m, the sample site reset rate should be greater than 98%, and the sample tree reset rate should be greater than 95%. Each period of forest resources inventory spans five years, and each province is surveyed separately. The data collected during forest resources surveys include a sample plot database and sample tree database, and all tree information in sample plots can be obtained from the sample tree database.

The sample plot database includes plot number, province, dominant species, average DBH, average tree height, longitude, latitude, altitude, soil thickness, slope, and other factors, while the sample tree database includes plot number, tree number, individual volume, and other factors. Among them, individual tree volume is consulted by the unitary volume table derived from the LY208-77 binary volume table [32]. It has a high accuracy, and we can regard it as a reference value.

In this study, we collected eighth national forest inventory data from 2009 to 2013, and after sorting the data, 4958 sample plots were obtained (Table 1). The stand volume, forest type, average DBH, average tree height, stand density, and forest basal area of 37 forest types were used to establish the model (Table S1). Among these variables, stand volume was the sum of all sample tree volumes in each sample plot, stand density was the sum of all trees in each sample plot, and forest basal area was calculated according to DBH and stand density. Because the shape and size of sample plots were different among the provinces, the volume of sample plots was converted according to one hectare (Table A1). The sample plots had high overall coverage in China and covered all provinces and cities (except Hong Kong, Macao, and Taiwan), which could reflect the status of forest resources in China (Figure 1).

**Table 1.** Statistical indicators of sample plots.

Factors	Number of Data Points ( $n = 4958$ )			
	Max	Min	Mean	SD
Stand Volume ( $\text{m}^3 \text{ha}^{-1}$ )	1142.61	0.06	104.91	106.63
Mean H (m)	40.30	0.40	11.63	5.31
Mean DBH (cm)	85.27	5.00	15.69	7.91
Stand Density ( $\text{tree ha}^{-1}$ )	6206.90	12.50	827.56	695.68

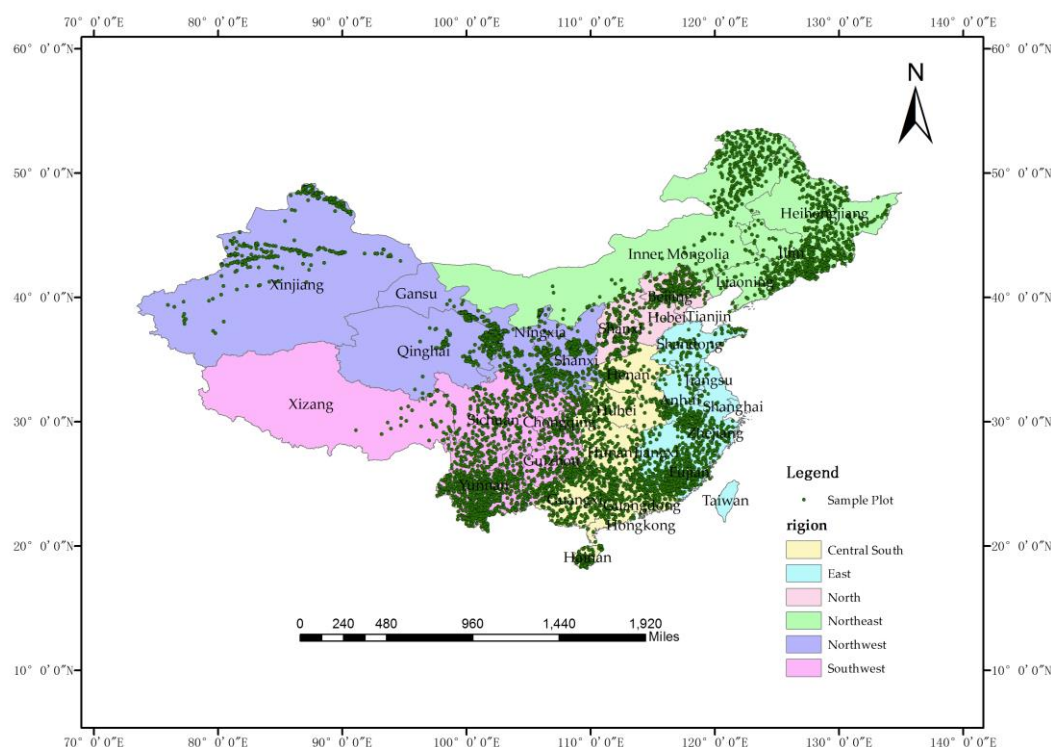


**Figure 1.** Regional Division and Forest Sample Distribution Map of China.

## 2.2. Method of Stand Volume Model Establishing

Tree height and DBH are important factors in forest resources survey, and are often used to predict stand productivity and volume. At the same time, the quantitative relationship between tree height

and DBH is also used to describe stand structure, analyze the stand growth of fixed sample plots, and formulate forest planning. Existing growth models have been used to overcome some of the difficulties associated with estimating or simulating the stand development of improved stock [33–36]. The accuracy of stand volume is highly dependent on the accuracy of the volume model.

Forest basal area is the main criterion reflecting site quality and an important factor for calculating stand volume, and it is related to average DBH and stand density [37]. Stand density is an index to evaluate the crowding degree among trees per unit area of forest, which directly affects environmental factors such as light, temperature, and humidity. It is an effective regulatory factor for forest management and has a significant impact on the composition and species diversity of undergrowth plants [38,39]. Therefore, in view of stand density and forest basal area, we established models for comparative analysis to obtain a more accurate model. To facilitate the practical use of the model and ensure the application value of the model, the volume model in this paper took the same form as the national binary volume model:  $V = ad^bH^c$  [40]. Given this theoretical basis, forests were divided into 37 types according to dominant tree species, and stand density was measured as tree number per unit area. A nonlinear stand volume model related to tree height, DBH, stand density, and forest basal area was established.

The formula for calculating the volume of the forest basal area is:

$$G = \frac{1}{4}\pi d^2 N, \quad (1)$$

where  $G$  is forest basal area ( $\text{m}^2 \text{ha}^{-1}$ ),  $d$  is the average DBH of the stand (cm), and  $N$  is the stand density (tree  $\text{ha}^{-1}$ ).

The two formulas for calculating the stand volume are as follows:

$$M_1 = ad^bH^cN^f, \quad (2)$$

$$M_2 = aH^bG^c, \quad (3)$$

where  $M_1$  and  $M_2$  are the stand volume ( $\text{m}^3 \text{ha}^{-1}$ ),  $H$  is the average height of stand (m), and  $a$ ,  $b$ , and  $c$  are parameters reflecting the stand volume.

To validate the two volume models and compare their advantages and disadvantages, we used the coefficient of determination ( $R^2$ ) and standard error (SE) [41]. Generally, when  $R^2$  approaches 1 and SE approaches 0, the fit is the optimal.

### 2.3. Model Evaluation and Validation

To validate the models, we examined the prediction accuracies achieved when estimating stand volume. Typically, models use an independent dataset or data derived from data splitting or bootstrapping procedures. To evaluate the model and its applicability, 80% of the samples were randomly selected to establish the model, which was evaluated by  $R^2$ , and the remaining 20% of the data were used for model validation [42]. Considering a variety of factors, we chose the following five indicators as the basic evaluation indicators: empirical coefficient of correlation ( $R_{\text{emp}}^2$ ), bias (BIAS), root mean square error (RMSE), relative bias (BIAS%), and RMSE (RMSE%).  $R_{\text{emp}}^2$  can assess the model, BIAS is the difference between the overall average value of a measurement or test result and the accepted reference value or true value, and RMSE, BIAS%, and RMSE% can reflect the precision of the model directly and clearly. The index expressions are as follows:

$$R_{\text{emp}}^2 = 1 - \frac{\sum (y_i - \hat{y}_i)^2}{\sum (y_i - \bar{y}_i)^2}, \quad (4)$$

$$\text{BIAS} = \frac{1}{n} \sum_{i=1}^n (y_i - \hat{y}_i), \quad (5)$$

$$RMSE = \sqrt{\sum (y_i - \hat{y}_i)^2 / (n - 1)}, \quad (6)$$

$$BIAS\% = \frac{BIAS}{\bar{y}_i} \times 100\%, \quad (7)$$

$$RMSE\% = \frac{RMSE}{\bar{y}_i} \times 100\%, \quad (8)$$

where  $y_i$  and  $\hat{y}_i$  are the measured values and predicted values of the sample plot ( $\text{m}^3 \text{ha}^{-1}$ ), respectively;  $\bar{y}_i$  is the average of the measured values of all sample plots ( $\text{m}^3 \text{ha}^{-1}$ ); and  $n$  is the number of sample plots.

#### 2.4. Methods of Aboveground Biomass (AGB) and Aboveground Carbon (AGC) Estimation

The response of terrestrial vegetation to a globally changing environment is central to predictions of future levels of atmospheric carbon dioxide [43]. In recent years, AGB and AGC estimation methods based on the re  $p_j$  and  $q_j$  are parameters of each species, and  $M$  is the stand volume ( $\text{m}^3 \text{ha}^{-1}$ ). Relationship between AGB and storage have been widely used [44]. In this study, the AGB of 37 forest types in China was estimated by the following linear regression equation [20], and the parameters are shown in Table 2.

$$B_j = p_j M + q_j, \quad (9)$$

where  $B_j$  is the AGB of forest type  $j$  ( $\text{Mg ha}^{-1}$ ),

**Table 2.** The conversion relations between stand volume and aboveground biomass (AGB).

Species	$p_j$	$q_j$
<i>Abies fabri</i> (Mast.) Craib	0.53	22.951
<i>Abrus</i> spp.	0.81	10.371
<i>Betula</i> spp.	0.82	18.08
<i>Betula Costata</i> Trautv	0.93	16.459
<i>Betula platyphylla</i> Suk.	1.33	−2.881
<i>Cryptomeria fortunei</i> Hooibrenk ex Otto et Dietr.	0.54	20.291
<i>Cunninghamia lanceolata</i> (Lamb.) Hook.	0.53	22.954
<i>Cupressus funebris</i> Endl.	0.54	46.846
<i>Eucalyptus robusta</i> Smith	0.87	1.531
<i>Keteleeria fortunei</i> (Murr.) Carr.	0.51	28.192
<i>Larix gmelinii</i> (Ruprecht) Kuzeneva	0.92	−12.64
Other hard-and-broad trees	0.96	29.083
Other pine trees	0.71	18.993
Other soft-and-broad trees	0.62	33.931
<i>Phoebe zhenman</i> S. Lee et F. N. Wei	0.89	28.353
<i>Picea asperata</i> Mast.	0.48	81.143
<i>Pinus armandii</i> Franch.	0.61	29.923
<i>Pinus densata</i> Mast.	0.81	11.892
<i>Pinus densiflora</i> Sieb. et Zucc.	0.72	15.982
<i>Pinus elliotii</i> Engelmann	0.68	19.759
<i>Pinus koraiensis</i> Siebold et Zuccarini	0.69	15.833
<i>Pinus massoniana</i> Lamb.	0.65	25.761
<i>Pinus tabulaeformis</i> Carr.	0.78	13.889
<i>Pinus taiwanensis</i> Hayata	0.91	8.919
<i>Pinus thunbergii</i> Parlatores	0.82	16.414
<i>Populus</i> spp.	0.72	24.932
<i>Quercus</i> spp.	0.96	43.056
<i>Robinia pseudoacacia</i> Linn.	1.14	7.2
<i>Salix</i> spp.	0.51	44.003
<i>Schima superba</i> Gardn. et Champ.	0.92	19.808
<i>Tilia tuan</i> Szyszyl.	0.68	54.484

The AGC of forest vegetation is usually calculated by using a 50% carbon content as a unified value, but this calculation may lead to large errors. In this paper, AGC was obtained by using the

following AGB–AGC conversion model of different species [45], and the parameters are shown in Table 3.

$$C_j = B_j C_c, \quad (10)$$

where  $C_j$  is the AGC of forest type  $j$  ( $\text{Mg ha}^{-1}$ ), and  $C_c$  is the carbon content of forest vegetation of each species (%).

**Table 3.** Carbon content in stands weighted by aboveground biomass (AGB).

Species	$C_c$ (%)	Species	$C_c$ (%)	Species	$C_c$ (%)	Species	$C_c$ (%)
A	52.59	F	52.11	J	51.6	N	50.19
B	54.37	G	53.65	K	49.56	O	48.32
C	51.44	H	54.79	L	50.41	P	50.5
D	52.16	I	50.5	M	49.38	Q	49.14
E	53.14						
coniferous forest	52.82	broad-leaved forest	49.37				
Average	51.09						

Note: A: *Populus* spp., B: *Pinus armandii* Franch., C: *Pinus massoniana* Lamb., D: *Pinus elliotii* Engelman, E: *Pinus tabulaeformis* Carr., F: *Cupressus funebris* Endl., G: *Cunninghamia lanceolata* (Lamb.) Hook., H: *Cryptomeria fortunei* Hooibrenk ex Otto et Dietr., I: *Abies fabri* (Mast.) Craib, J: *Picea asperata* Mast., K: *Larix gmelinii* (Ruprecht) Kuzeneva, L: *Betula Costata* Trautv, M: *Betula* spp., N: *Eucalyptus robusta* Smith, O: *Quercus* spp., P: *Phoebe zhennan* S. Lee et F. N. Wei, Q: *Cinnamomum camphora* (L.) Presl.

### 3. Results

#### 3.1. Result of Stand Volume Model Establishment

Two models ( $M_1 = ad^b H^c N^f$ ,  $M_2 = aH^b G^c$ ) were established for each forest type by using 80% of the data. Among the 37 forest types, 31 forest types exhibited an  $R^2$  greater than 0.8 for model 1, and 36, for model 2, which indicated that the two models well represented the natural growth process of each type of forest, and model  $M_2 = aH^b G^c$  (Table 4) was better than model  $M_1 = ad^b H^c N^f$  (Table 5).

**Table 4.** Fitting results for model 1.

Forest Type	n	$M_1 = ad^b H^c N^f$								$R^2$
		a	SE(a)	b	SE(b)	c	SE(c)	f	SE(f)	
<i>Abies fabri</i> (Mast.) Craib	72	0.064	0.056	1.259	0.178	0.311	0.152	0.592	0.078	0.77
<i>Abrus</i> spp.	8	0.026	0.065	1.094	0.715	0.946	0.696	0.438	0.292	0.98
<i>Betula</i> spp.	98	0.004	0.002	1.938	0.090	0.078	0.086	0.706	0.041	0.89
<i>Betula Costata</i> Trautv	14	0.005	0.007	1.921	0.231	0.010	0.367	0.681	0.131	0.97
<i>Betula platyphylla</i> Suk.	206	0.051	0.021	1.158	0.094	0.340	0.075	0.508	0.037	0.76
<i>Cryptomeria fortunei</i> Hooibrenk ex Otto et Dietr.	9	0.093	0.195	1.499	0.326	0.070	0.062	0.461	0.173	0.91
<i>Cunninghamia lanceolata</i> (Lamb.) Hook.	318	0.022	0.004	1.703	0.056	0.048	0.024	0.575	0.023	0.86
<i>Cupressus funebris</i> Endl.	219	0.006	0.002	1.633	0.065	0.419	0.054	0.646	0.035	0.87
<i>Eucalyptus robusta</i> Smith	90	0.010	0.005	1.568	0.146	0.186	0.068	0.650	0.044	0.87
<i>Keteleeria fortunei</i> (Murr.) Carr.	182	2.311	6.804	0.010	0.970	0.788	0.609	0.254	0.208	0.55
<i>Larix gmelinii</i> (Ruprecht) Kuzeneva	294	0.012	0.003	1.396	0.070	0.492	0.056	0.627	0.033	0.84
<i>Cinnamomum camphora</i> (L.) Presl.	4	0.188	2.191	1.904	1.513	0.001	1.865	0.134	1.508	0.96
Other hard-and-broad trees	134	0.005	0.001	2.066	0.098	0.194	0.150	0.561	0.066	0.80
Other pine trees	8	0.032	0.044	1.686	0.233	0.509	0.162	0.319	0.175	0.98



Table 4. Cont.

Forest Type	n	$M_1 = ad^b H^c N^f$								
		a	SE(a)	b	SE(b)	c	SE(c)	f	SE(f)	R <sup>2</sup>
Other soft-and-broad trees	87	0.098	0.060	1.210	0.126	0.482	0.146	0.355	0.059	0.89
<i>Phoebe zhennan</i> S. Lee et F. N. Wei	6	0.013	0.070	1.447	1.203	0.863	0.729	0.542	0.538	0.83
<i>Picea asperata</i> Mast.	479	0.051	0.013	1.425	0.06	0.269	0.05	0.522	0.023	0.84
<i>Pinus armandii</i> Franch.	29	0.015	0.012	1.072	0.225	0.666	0.164	0.609	0.063	0.90
<i>Pinus densata</i> Mast.	64	0.348	0.375	0.014	0.319	1.578	0.246	0.333	0.085	0.91
<i>Pinus densiflora</i> Sieb. et Zucc.	11	0.008	0.013	1.206	0.373	0.863	0.188	0.552	0.146	0.96
<i>Pinus elliotii</i> Engelman	22	0.043	0.058	1.365	0.321	0.069	0.083	0.513	0.115	0.80
<i>Pinus kesiya</i> Royle ex Gordon var. <i>langbianensis</i> (A.Chev) Gaussen	28	0.749	2.117	0.888	0.467	0.040	0.230	0.391	0.169	0.47
<i>Pinus koraiensis</i> Siebold et Zuccarini	8	0.054	0.185	0.556	0.932	1.312	0.672	0.415	0.330	0.89
<i>Pinus massoniana</i> Lamb.	336	0.014	0.006	1.559	0.074	0.184	0.045	0.603	0.027	0.83
<i>Pinus sylvestris</i> Linn. var. <i>mongolica</i> Litv.	14	0.084	0.088	0.438	0.268	1.328	0.239	0.376	0.093	0.90
<i>Pinus tabulaeformis</i> Carr.	11	0.011	0.004	1.089	0.095	0.821	0.064	0.614	0.031	0.90
<i>Pinus taiwanensis</i> Hayata	4	0.322	2.247	0.605	1.976	1.111	1.972	0.236	0.715	0.97
<i>Pinus thunbergii</i> Parlatore	14	0.022	0.032	1.274	0.464	0.545	0.303	0.529	0.137	0.88
<i>Pinus yunnanensis</i> Franch.	184	0.072	0.017	0.778	0.158	1.253	0.111	0.354	0.044	0.89
<i>Populus</i> spp.	296	0.015	0.009	1.533	0.071	0.194	0.072	0.627	0.032	0.77
<i>Quercus</i> spp.	578	0.011	0.003	1.555	0.059	0.286	0.050	0.626	0.024	0.82
<i>Robinia pseudoacacia</i> Linn.	39	0.004	0.002	1.761	0.133	0.069	0.132	0.750	0.065	0.90
<i>Salix</i> spp.	36	0.005	0.004	1.591	0.199	0.301	0.126	0.688	0.085	0.87
<i>Schima superba</i> Gardn. et Champ.	16	0.051	0.064	1.168	0.376	0.551	0.242	0.429	0.123	0.92
<i>Tilia tuan</i> Szyszyl.	18	0.003	0.004	1.509	0.459	0.968	0.394	0.559	0.142	0.91
<i>Tsuga chinensis</i> (Franch.) Pritz.	6	0.171	0.328	1.231	1.449	0.995	1.149	0.029	0.134	0.94
<i>Ulmus pumila</i> Linn.	27	0.002	0.002	1.363	0.265	0.833	0.185	0.711	0.102	0.84

Table 5. Fitting results for model 2.

Forest Type	n	$M_2 = aH^b G^c$						
		a	SE(a)	b	SE(b)	c	SE(c)	R <sup>2</sup>
<i>Abies fabri</i> (Mast.) Craib	72	5.678	1.726	1.033	0.103	0.278	0.061	0.86
<i>Abrus</i> spp.	8	3.439	2.612	0.863	0.493	0.385	0.240	0.99
<i>Betula</i> spp.	98	1.880	0.267	1.065	0.067	0.436	0.044	0.91
<i>Betula Costata</i> Trautv	14	1.851	0.421	1.257	0.137	0.237	0.119	0.98
<i>Betula platyphylla</i> Suk.	206	3.540	0.518	0.861	0.057	0.369	0.035	0.83
<i>Cryptomeria fortunei</i> Hooibrenk ex Otto et Dietr.	9	6.635	5.739	1.030	0.078	0.003	0.247	0.88
<i>Cunninghamia lanceolata</i> (Lamb.) Hook.	318	3.966	0.288	1.032	0.021	0.134	0.021	0.91
<i>Cupressus funebris</i> Endl.	219	2.218	0.205	1.076	0.045	0.334	0.030	0.92
<i>Eucalyptus robusta</i> Smith	90	3.434	0.380	0.992	0.042	0.226	0.033	0.94
<i>Keteleeria fortunei</i> (Murr.) Carr.	184	2.055	0.952	0.842	0.131	0.696	0.117	0.91
<i>Larix gmelinii</i> (Ruprecht) Kuzeneva	294	2.524	0.472	0.911	0.050	0.535	0.033	0.88
<i>Cinnamomum camphora</i> (L.) Presl.	4	3.760	15.418	0.953	1.558	0.346	0.862	0.95
Other hard-and-broad trees	134	0.462	0.140	1.299	0.134	0.741	0.058	0.82

Table 5. Cont.

Forest Type	n	$M_2 = aH^b G^c$						$R^2$
		a	SE(a)	b	SE(b)	c	SE(c)	
Other pine trees	8	1.743	0.457	1.143	0.111	0.332	0.091	0.99
Other soft-and-broad trees	87	2.090	0.667	0.860	0.140	0.639	0.086	0.92
<i>Phoebe zhenan</i> S. Lee et F. N. Wei	6	0.131	0.050	1.521	0.089	1.156	0.090	0.99
<i>Picea asperata</i> Mast.	479	3.550	0.307	0.816	0.032	0.592	0.023	0.88
<i>Pinus armandii</i> Franch.	29	2.572	0.442	0.826	0.074	0.537	0.037	0.96
<i>Pinus densata</i> Mast.	64	2.918	0.393	0.936	0.056	0.582	0.054	0.97
<i>Pinus densiflora</i> Sieb. et Zucc.	11	1.335	0.344	0.921	0.122	0.682	0.131	0.98
<i>Pinus elliotii</i> Engelman	22	3.099	0.496	1.077	0.034	0.110	0.060	0.95
<i>Pinus kesiya</i> Royle ex Gordon var. <i>langbianensis</i> (A.Chev) Gaussen	28	5.598	3.531	0.829	0.147	0.346	0.140	0.65
<i>Pinus koraiensis</i> Siebold et Zuccarini	8	1.052	0.532	0.953	0.147	0.800	0.113	0.96
<i>Pinus massoniana</i> Lamb.	336	2.694	0.243	0.949	0.032	0.371	0.024	0.87
<i>Pinus sylvestris</i> Linn. var. <i>mongolica</i> Litv.	14	2.154	0.971	0.431	0.180	1.036	0.105	0.89
<i>Pinus tabulaeformis</i> Carr.	11	2.027	0.183	0.837	0.042	0.623	0.028	0.93
<i>Pinus taiwanensis</i> Hayata	4	2.062	0.834	0.957	0.346	0.506	0.320	0.99
<i>Pinus thunbergii</i> Parlato	14	1.681	0.276	1.025	0.077	0.497	0.058	0.98
<i>Pinus yunnanensis</i> Franch.	182	1.097	0.134	0.734	0.040	1.141	0.035	0.92
<i>Populus</i> spp.	296	3.797	0.291	1.032	0.043	0.217	0.028	0.81
<i>Quercus</i> spp.	578	2.204	0.166	1.018	0.031	0.423	0.021	0.88
<i>Robinia pseudoacacia</i> Linn.	39	2.727	0.516	1.081	0.081	0.251	0.051	0.95
<i>Salix</i> spp.	36	3.997	0.546	1.159	0.067	0.029	0.058	0.95
<i>Schima superba</i> Gardn. et Champ.	16	3.729	1.065	0.785	0.161	0.424	0.110	0.94
<i>Tilia tuan</i> Szyszyl.	18	0.900	0.324	1.079	0.210	0.697	0.123	0.96
<i>Tsuga chinensis</i> (Franch.) Pritz.	6	0.945	2.057	0.087	0.755	1.904	0.098	0.93
<i>Ulmus pumila</i> Linn.	27	1.376	0.485	0.888	0.164	0.740	0.101	0.89

### 3.2. Model Precision Evaluation

To obtain the precision for the different modeled forest types, 20% of the samples were used for data validation. BIAS, BIAS%, RMSE, RMSE% and  $R^2_{\text{emp}}$  were used as indicators for precision testing (Tables 6 and 7). As shown in Table 6 for model 1, most BIAS values were near 0; the average BIAS% and RMSE% were 4.014% and 26.826%, respectively; the average  $R^2_{\text{emp}}$  was 0.86; and 30 of 37 forest types had an  $R^2_{\text{emp}}$  more than 0.8. As shown in Table 7 for model 2, BIAS values were all near 0; the average BIAS% and RMSE% were 0.693% and 20.178%, respectively; the average  $R^2_{\text{emp}}$  value was 0.91; and 35 of 37 forest types had an  $R^2_{\text{emp}}$  greater than 0.8. These results indicated that the two models were relatively stable and could be used to estimate stand volume. By comparison, model 1 had higher fitting accuracy and achieved better estimate precision.

We chose eight largest forest types as examples to make comparison between the predicted value and the observed value (Figure 2). The residual can be obtained from this equation and can be used to evaluate the uniformity and normality. The results showed that the residuals were homogeneously distributed, meaning that they had no heterogeneity, which conformed to the general law of error distribution [46].

As shown in Figure 2, the predicted value and the observed value of each forest types were linearly fitted; the linear relationship is shown by the red line, and that the  $R^2$  value was greater than 0.94.



The slope of each forest type was close to 1, showing that the predicted and observed values were not significantly different.

**Table 6.** Validation of the stand volume precision of model 1 for different forest types.

Forest Type	$M_1 = ad^b H^c N^f$					
	<i>n</i>	BIAS	BIAS%	RMSE	RMSE%	$R^2_{emp}$
<i>Abies fabri</i> (Mast.) Craib	18	−4.631	−1.469	108.468	34.410	0.77
<i>Abrus</i> spp.	2	−0.979	−1.514	11.599	17.939	0.96
<i>Betula</i> spp.	25	−10.237	−16.852	17.126	28.192	0.93
<i>Betula Costata</i> Trautv	3	−6.334	−10.697	12.197	20.600	0.97
<i>Betula platyphylla</i> Suk.	51	−1.307	−2.147	16.707	27.443	0.76
<i>Cryptomeria fortunei</i> Hooibrenk ex Otto et Dietr.	2	−5.437	−3.107	31.240	17.849	0.91
<i>Cunninghamia lanceolata</i> (Lamb.) Hook.	79	−10.321	−10.936	27.063	28.675	0.88
<i>Cupressus funebris</i> Endl.	55	−11.859	−17.978	22.442	34.023	0.89
<i>Eucalyptus robusta</i> Smith	22	−0.391	−0.722	14.273	26.371	0.88
<i>Keteleeria fortunei</i> (Murr.) Carr.	48	−0.339	−0.559	16.632	27.427	0.54
<i>Larix gmelinii</i> (Ruprecht) Kuzeneva	73	−5.841	−8.216	28.093	39.518	0.79
<i>Cinnamomum camphora</i> (L.) Presl.	1	−2.543	−3.228	14.319	18.173	0.96
Other hard-and-broad trees	33	3.048	5.391	34.443	60.914	0.82
Other pine trees	2	−3.910	−5.821	9.020	13.427	0.98
Other soft-and-broad trees	22	−4.721	−6.553	19.045	26.434	0.69
<i>Phoebe zhenan</i> S. Lee et F. N. Wei	1	−38.301	−17.039	101.687	45.236	0.84
<i>Picea asperata</i> Mast.	120	−7.283	−3.593	56.124	27.688	0.84
<i>Pinus armandii</i> Franch.	7	1.655	2.547	12.974	19.961	0.96
<i>Pinus densata</i> Mast.	16	−0.278	−0.107	35.021	13.479	0.91
<i>Pinus densiflora</i> Sieb. et Zucc.	3	0.147	0.752	4.024	20.512	0.96
<i>Pinus elliotii</i> Engelmann	5	−0.615	−1.418	11.488	26.493	0.80
<i>Pinus kesiya</i> Royle ex Gordon var. <i>langbianensis</i> (A.Chev) Gausson	7	−0.170	−0.133	30.147	23.520	0.39
<i>Pinus koraiensis</i> Siebold et Zuccarini	2	−2.533	−1.975	31.033	24.197	0.89
<i>Pinus massoniana</i> Lamb.	84	−0.694	−1.026	18.405	27.210	0.82
<i>Pinus sylvestris</i> Linn. var. <i>mongolica</i> Litv.	3	0.232	0.243	19.212	20.097	0.91
<i>Pinus tabulaeformis</i> Carr.	3	−5.454	−8.909	15.139	24.730	0.90
<i>Pinus taiwanensis</i> Hayata	1	−1.720	−1.707	14.397	14.292	0.97
<i>Pinus thunbergii</i> Parlatores	3	−3.351	−6.567	13.240	25.945	0.88
<i>Pinus yunnanensis</i> Franch.	44	−3.162	−2.223	41.252	29.011	0.90
<i>Populus</i> spp.	74	−9.204	−7.402	36.749	29.557	0.82
<i>Quercus</i> spp.	144	−4.219	−5.780	26.319	36.063	0.82
<i>Robinia pseudoacacia</i> Linn.	10	−4.830	−14.251	8.243	24.323	0.92
<i>Salix</i> spp.	9	2.326	4.102	19.431	34.261	0.89
<i>Schima superba</i> Gardn. et Champ.	4	−1.104	−2.481	9.067	20.373	0.92
<i>Tilia tuan</i> Szyszyl.	4	−1.906	−3.392	14.126	25.136	0.91
<i>Tsuga chinensis</i> (Franch.) Pritz.	2	−6.390	−2.085	69.846	22.795	0.94
<i>Ulmus pumila</i> Linn.	7	2.612	8.343	11.359	36.280	0.88

**Table 7.** Validation of stand volume precision of model 2 for different forest types.

Forest Type	$M_2 = aH^bG^c$					
	<i>n</i>	BIAS	BIAS%	RMSE	RMSE%	$R^2_{emp}$
<i>Abies fabri</i> (Mast.) Craib	18	3.856	1.223	82.991	26.328	0.86
<i>Abrus</i> spp.	2	−0.600	−0.928	8.563	13.243	0.98
<i>Betula</i> spp.	25	0.882	1.452	15.546	25.591	0.91
<i>Betula Costata</i> Trautv	3	0.829	1.401	9.201	15.539	0.98
<i>Betula platyphylla</i> Suk.	51	0.707	1.162	14.184	23.298	0.83
<i>Cryptomeria fortunei</i> Hooibrenk ex Otto et Dietr.	2	−1.057	−0.604	36.320	20.751	0.88
<i>Cunninghamia lanceolata</i> (Lamb.) Hook.	79	−0.121	−0.128	22.357	23.688	0.91
<i>Cupressus funebris</i> Endl.	55	−0.112	−0.170	17.710	26.849	0.92
<i>Eucalyptus robusta</i> Smith	22	0.126	0.234	10.057	18.581	0.94
<i>Keteleeria fortunei</i> (Murr.) Carr.	48	−0.031	−0.051	7.434	12.259	0.91
<i>Larix gmelinii</i> (Ruprecht) Kuzeneva	73	1.501	2.112	25.544	35.933	0.81
<i>Cinnamomum camphora</i> (L.) Presl.	1	−1.269	−1.611	15.434	19.588	0.95
Other hard-and-broad trees	33	10.573	18.699	32.778	57.970	0.82
Other pine trees	2	−0.047	−0.070	5.672	8.442	0.99
Other soft-and-broad trees	22	−0.053	−0.074	16.356	22.702	0.65
<i>Phoebe zhennan</i> S. Lee et F. N. Wei	1	1.504	0.669	12.534	5.576	1.00
<i>Picea asperata</i> Mast.	120	3.522	1.738	49.291	24.317	0.88
<i>Pinus armandii</i> Franch.	7	−0.247	−0.380	7.716	11.871	0.95
<i>Pinus densata</i> Mast.	16	−0.254	−0.098	21.830	8.402	0.97
<i>Pinus densiflora</i> Sieb. et Zucc.	3	0.111	0.567	2.767	14.106	0.98
<i>Pinus elliotii</i> Engelmann	5	0.156	0.360	5.645	13.019	0.95
<i>Pinus kesiya</i> Royle ex Gordon var. <i>langbianensis</i> (A.Chev) Gaussen	7	0.186	0.145	24.464	19.086	0.55
<i>Pinus koraiensis</i> Siebold et Zuccarini	2	−0.489	−0.381	17.280	13.474	0.97
<i>Pinus massoniana</i> Lamb.	84	0.647	0.956	15.811	23.376	0.87
<i>Pinus sylvestris</i> Linn. var. <i>mongolica</i> Litv.	3	−0.122	−0.128	20.878	21.840	0.89
<i>Pinus tabulaeformis</i> Carr.	3	−0.290	−0.474	12.692	20.733	0.93
<i>Pinus taiwanensis</i> Hayata	1	0.187	0.185	5.334	5.295	1.00
<i>Pinus thunbergii</i> Parlatore	3	−0.133	−0.261	4.757	9.321	0.98
<i>Pinus yunnanensis</i> Franch.	44	0.903	0.635	33.800	23.770	0.93
<i>Populus</i> spp.	74	1.233	0.992	32.559	26.187	0.88
<i>Quercus</i> spp.	144	0.070	0.096	21.501	29.461	0.88
<i>Robinia pseudoacacia</i> Linn.	10	−0.212	−0.625	5.891	17.382	0.95
<i>Salix</i> spp.	9	0.533	0.940	11.984	21.131	0.95
<i>Schima superba</i> Gardn. et Champ.	4	−0.347	−0.780	7.396	16.618	0.94
<i>Tilia tuan</i> Szyszyl.	4	0.232	0.414	9.135	16.255	0.96
<i>Tsuga chinensis</i> (Franch.) Pritz.	2	−2.609	−0.851	75.815	24.744	0.93
<i>Ulmus pumila</i> Linn.	7	−0.226	−0.723	9.345	29.847	0.89

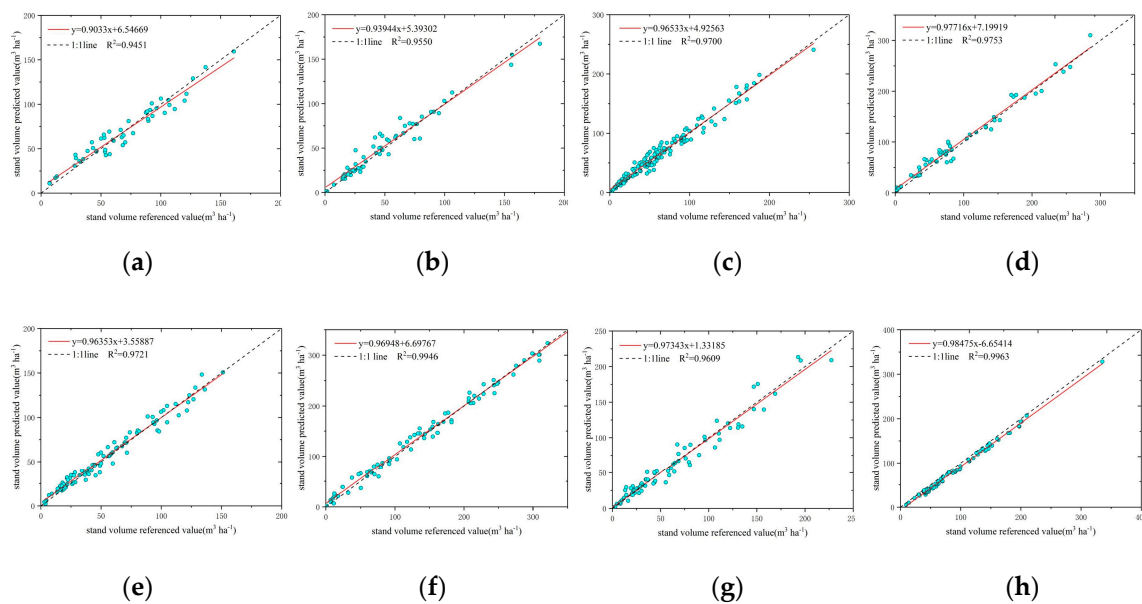


**Figure 2.** Referenced and predicted values of stand volume plotted, for *Betula platyphylla* Suk. (a), *Cupressus funebris* Endl. (b), *Quercus* spp. (c), *Populus* (d), *Pinus massoniana* Lamb. (e), *Picea asperata* Mast. (f), *Larix gmelinii* (Ruprecht) Kuzeneva (g), and *Cunninghamia lanceolata* (Lamb.) Hook. (h).

### 3.3. Results of Aboveground Biomass (AGB) and Aboveground Carbon (AGC) for Different Forest Types in China

We identified 37 main types of arbor forest (dominant species) in the eighth national forest resources inventory. According to Formulas (9) and (10), the AGB, AGC, AGB density, and AGC density of each arbor forest type were estimated (Table 8).

**Table 8.** Aboveground biomass (AGB), AGB density, aboveground carbon (AGC) and AGC density of each forest type.

Forest Type	Area (ha <sup>-1</sup> )	AGB (Mg)	AGB Density (Mg ha <sup>-1</sup> )	AGC (Mg)	AGC Density (Mg ha <sup>-1</sup> )
<i>Abies fabri</i> (Mast.) Craib	121	21,630.88	178.77	10,923.59	90.28
<i>Abrus</i> spp.	10	615.75	61.57	307.87	30.79
<i>Betula</i> spp.	136	9899.58	72.79	4888.41	35.94
<i>Betula Costata</i> Trautv	17	1215.93	71.53	600.42	35.32
<i>Betula platyphylla</i> Suk.	247	20,531.92	83.13	10,138.66	41.05
<i>Cryptomeria fortunei</i> Hooibrenk ex Otto et Dietr.	11	1262.85	114.80	691.92	62.90
<i>Cunninghamia lanceolata</i> (Lamb.) Hook.	397	28,970.88	72.97	15,542.88	39.15
<i>Cupressus funebris</i> Endl.	310	25,764.39	83.11	13,425.82	43.31
<i>Eucalyptus robusta</i> Smith	103	5394.36	52.37	2707.43	26.29
<i>Keteleeria fortunei</i> (Murr.) Carr.	15	898.67	59.91	449.34	29.96
<i>Larix gmelinii</i> (Ruprecht) Kuzeneva	370	28,162.67	76.12	13,957.42	37.72
<i>Cinnamomum camphora</i> (L.) Presl.	5	523.61	104.72	257.30	51.46
Other hard-and-broad trees	167	13,869.28	83.05	6934.64	41.52
Other pine trees	10	666.91	66.69	333.45	33.35
Other soft-and-broad trees	138	11,447.67	82.95	5723.84	41.48
<i>Phoebe zhenan</i> S. Lee et F. N. Wei	7	1598.92	228.42	807.45	115.35
<i>Picea asperata</i> Mast.	669	120,088.36	179.50	61,917.56	92.55

Table 8. Cont.

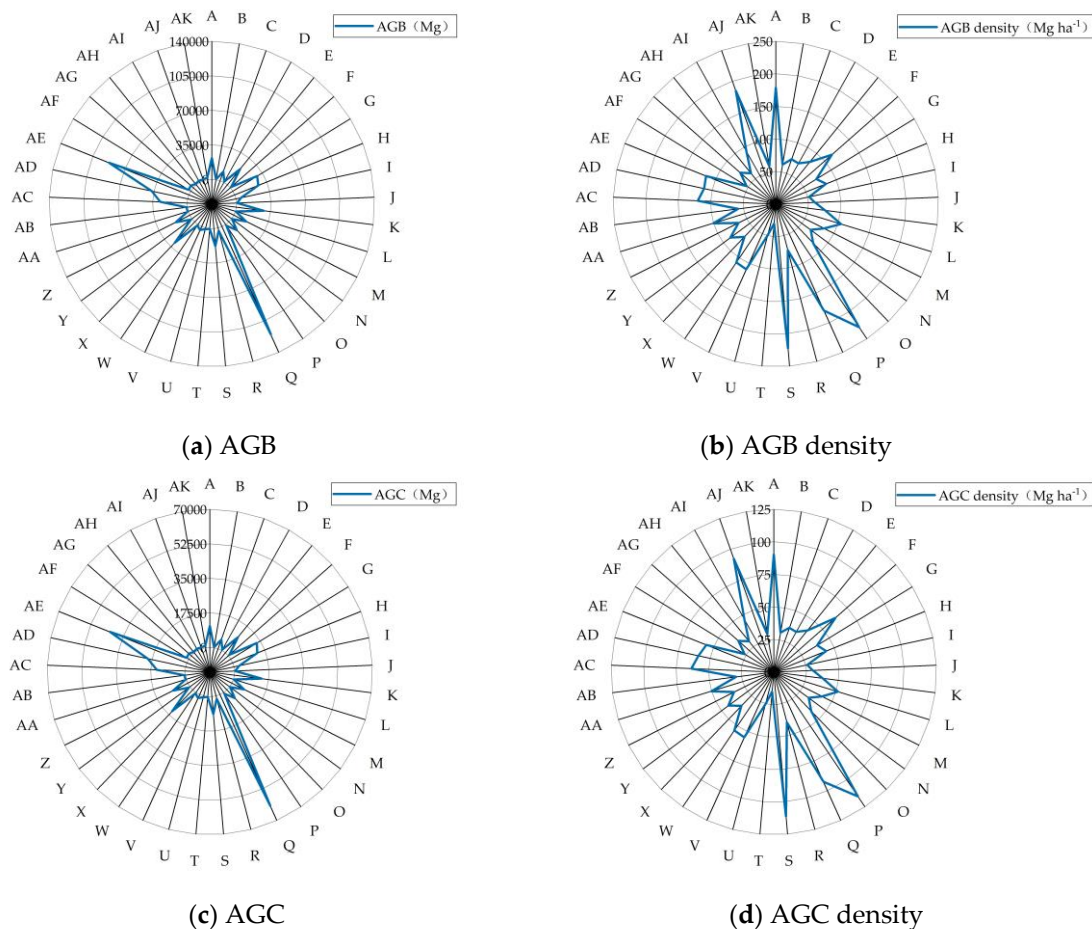
Forest Type	Area (ha <sup>-1</sup> )	AGB (Mg)	AGB Density (Mg ha <sup>-1</sup> )	AGC (Mg)	AGC Density (Mg ha <sup>-1</sup> )
<i>Pinus armandii</i> Franch.	39	2859.77	73.33	1554.86	39.87
<i>Pinus densata</i> Mast.	80	17,787.37	222.34	8893.69	111.17
<i>Pinus densiflora</i> Sieb. et Zucc.	14	421.49	30.11	210.75	15.05
<i>Pinus elliottii</i> Engelman	27	1329.63	49.25	693.53	25.69
<i>Pinus kesiya</i> Royle ex Gordon var. <i>langbianensis</i> (A.Chev) Gaussen	35	3849.93	110.00	1924.96	55.00
<i>Pinus koraiensis</i> Siebold et Zuccarini	10	1081.73	108.17	540.87	54.09
<i>Pinus massoniana</i> Lamb.	420	29,285.55	69.73	15,064.48	35.87
<i>Pinus sylvestris</i> Linn. var. <i>mongolica</i> Litv.	17	1476.73	86.87	738.36	43.43
<i>Pinus tabulaeformis</i> Carr.	246	15,819.99	64.31	8406.74	34.17
<i>Pinus taiwanensis</i> Hayata	5	502.96	100.59	251.48	50.30
<i>Pinus thunbergii</i> Parlato	17	990.39	58.26	495.19	29.13
<i>Pinus yunnanensis</i> Franch.	228	27,349.17	119.95	14,443.10	63.35
<i>Populus</i> spp.	332	37,392.68	112.63	19,664.81	59.23
<i>Quercus</i> spp.	754	87,208.34	115.66	42,139.07	55.89
<i>Robinia pseudoacacia</i> Linn.	48	2527.81	52.66	1263.91	26.33
<i>Salix</i> spp.	45	3281.71	72.93	1626.42	36.14
<i>Schima superba</i> Gardn. et Champ.	20	1215.04	60.75	607.52	30.38
<i>Tilia tuan</i> Szyszyl.	22	2039.34	92.70	1019.67	46.35
<i>Tsuga chinensis</i> (Franch.) Pritz.	8	1475.66	184.46	737.83	92.23
<i>Ulmus pumila</i> Linn.	34	2010.73	59.14	1005.37	29.57

The total AGB and AGC obtained from the survey data were 532,448.64 Mg and 270,890.61 Mg, respectively, and the average AGB density and AGC density of the forest types were 95.03 Mg ha<sup>-1</sup> and 48.15 Mg ha<sup>-1</sup>, respectively. Pearson correlation coefficients obtained by correlation analysis revealed a strong correlation between AGB (AGB density) and AGC (AGC density), and the change trends of AGB (AGB density) and AGC (AGC density) for each forest type were basically the same (Table 9) (Figure 3). The forest types can be divided into coniferous forest and broad-leaved forest (Table A2). Coniferous forest AGB and AGC accounted for 64.0% and 65.3% of the total, while broad-leaved forest AGB and AGC accounted for 36.0% and 34.7% of the total, respectively. The AGB and AGC of *Picea asperata* Mast., *Quercus* spp., and *Populus* spp. were the highest among the forest types, accounting for 50% of the total AGB and 45.7% of the total AGC. The AGB and AGC of *Cinnamomum camphora* (L.) Presl., *Pinus taiwanensis* Hayata, and *Pinus densiflora* Sieb. et Zucc. were the lowest, accounting for only 0.3% of the total AGB and AGC. The 10 forest types with the smallest area accounted for approximately 1.5% of the total AGB and AGC, while the 10 forest types with the largest area accounted for approximately 79%. Because the areas of the sample plots in this study were different and the data used were part of the eighth forest resources inventory, the AGB density and AGC density may better represent the actual situation of each forest type in China. The average AGB density and AGC density of coniferous forest were 102.18 Mg ha<sup>-1</sup> and 52.38 Mg ha<sup>-1</sup>, and the average AGB density and AGC density of broad-leaved forest were 85.66 Mg ha<sup>-1</sup> and 42.60 Mg ha<sup>-1</sup>, respectively. For forest types, the AGB and AGC density were quite different. The AGB and AGC density of *Phoebe zhennan* S. Lee et F. N. Wei and *Pinus densata* Mast. were the highest, while those of *Pinus densiflora* Sieb. et Zucc., *Pinus elliottii* Engelman, and *Eucalyptus robusta* Smith were the lowest. The maximum AGB density and AGC density were 7.59 and 7.66 times of the minimum, respectively.

**Table 9.** Correlation coefficients between aboveground biomass (AGB) (AGB density) and aboveground carbon (AGC) (AGC density).

		AGC	AGC Density
AGB	Pearson correlation coefficient	0.999 **	
	Significance	0.000	
AGB Density	Pearson correlation coefficient		0.998 **
	Significance		0.000

Note: \*\* indicates a significant correlation at 0.01 level.

**Figure 3.** Quantitative differences among forest types. (a–d) show radar charts of aboveground biomass (AGB), AGB density, aboveground carbon (AGC) and AGC density, respectively, for A: *Abies fabri* (Mast.) Craib, B: *Abrus* spp., C: *Betula* spp., D: *Betula Costata* Trautv, E: *Betula platyphylla* Suk., F: *Cryptomeria fortunei* Hooibrenk ex Otto et Dietr., G: *Cunninghamia lanceolata* (Lamb.) Hook., H: *Cupressus funebris* Endl., I: *Eucalyptus robusta* Smith, J: *Keteleeria fortunei* (Murr.) Carr., K: *Larix gmelinii* (Ruprecht) Kuzeneva, L: *Cinnamomum camphora* (L.) Presl, M: Other hard-and-broad trees, N: Other pine trees, O: Other soft-and-broad trees, P: *Phoebe zhenan* S. Lee et F. N. Wei, Q: *Picea asperata* Mast., R: *Pinus armandii* Franch., S: *Pinus densata* Mast., T: *Pinus densiflora* Sieb. et Zucc., U: *Pinus elliotii* Engelmann, V: *Pinus kesiya* Royle ex Gordon var. *langbianensis* (A.Chev) Gaussen, W: *Pinus koraiensis* Siebold et Zuccarini, X: *Pinus massoniana* Lamb., Y: *Pinus sylvestris* Linn. var. *mongolica* Litv., Z: *Pinus tabulaeformis* Carr., AA: *Pinus taiwanensis* Hayata, AB: *Pinus thunbergii* Parlatores, AC: *Pinus yunnanensis* Franch., AD: *Populus* spp., AE: *Quercus* spp., AF: *Robinia pseudoacacia* Linn., AG: *Salix* spp., AH: *Schima superba* Gardn. et Champ., AI: *Tilia tuan* Szyszyl, AJ: *Tsuga chinensis* (Franch.) Pritz. and AK: *Ulmus pumila* Linn.

### 3.4. Spatial Distribution of Forest Aboveground Biomass (AGB) and Aboveground Carbon (AGC) in China

To intuitively understand the spatial distribution of AGC density, the kriging interpolation method was used to map the distribution of AGC density in China (Figure 4). As shown in the figure, the AGC density in eastern China is generally lower than that in western China; thus, AGC density should be analyzed separately among regions. The goal of regional division is to divide the whole territory of a country into several blocks according to their characteristics, in order to study and manage geography, the climate, the economy, and administration. According to the most far-reaching and widely used method, 34 provincial administrative regions in China can be divided into six regions: northwest (Shaanxi, Gansu, Qinghai, Ningxia, and Xinjiang), north (Beijing, Tianjin, Hebei, and Shanxi), northeast (Liaoning, Jilin, Heilongjiang, and Inner Mongolia), east (Shanghai, Jiangsu, Zhejiang, Anhui, Fujian, Jiangxi, Shandong, and Taiwan), central south (Henan, Hubei, Hunan, Guangdong, Guangxi, Hainan, Hong Kong, and Macao) and southwest (Sichuan, Guizhou, Yunnan, Chongqing, and Xizang). Based on the data above, the AGB, AGC, AGB density, and AGC density of the six regional types can be obtained (Table 10).

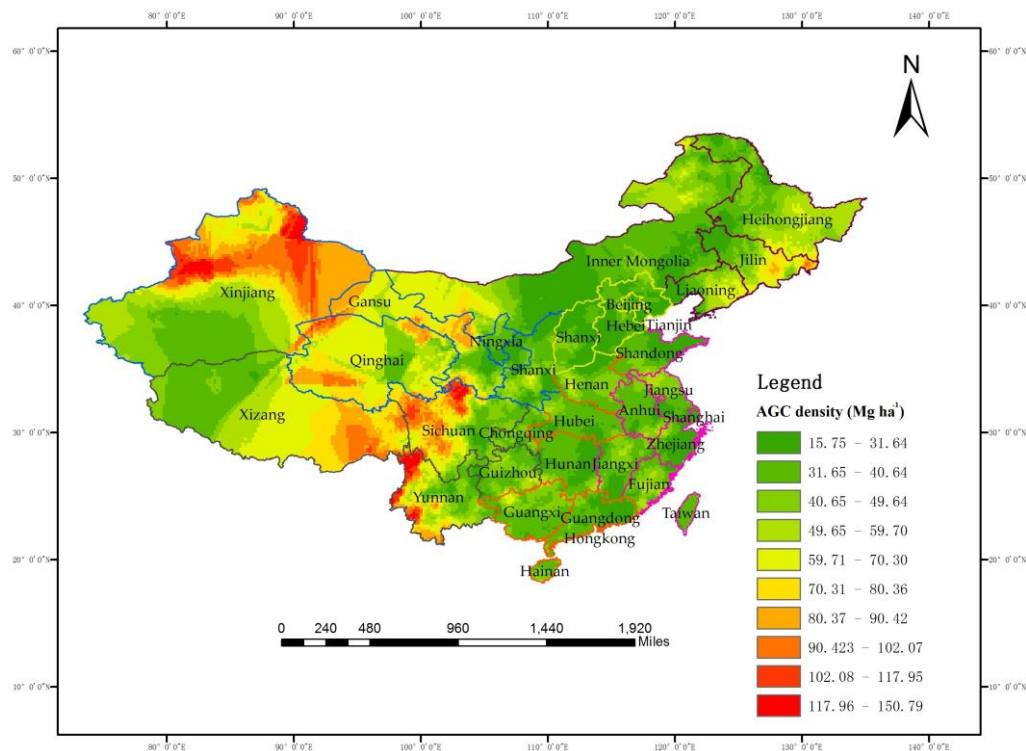


Figure 4. Aboveground carbon (AGC) density distribution in China.

Table 10. Aboveground biomass (AGB) and aboveground carbon (AGC) in different regions of China.

Region	AGB (Mg)	AGB Density (Mg ha <sup>-1</sup> )	AGC (Mg)	AGC Density (Mg ha <sup>-1</sup> )
Northeast	47,114.60	90.09	23,598.57	45.12
North	33,124.63	64.70	16,631.47	32.48
East	34,205.09	71.41	17,633.56	36.81
Central South	43,582.00	71.21	22,290.98	36.42
Southwest	169,050.87	131.25	85,909.11	66.70
Northwest	205,371.44	119.40	104,826.92	60.95

The AGB and AGC of arbor forests among these regions in China range from high to low are as follows: northwest, southwest, northeast, central south, east, and north (Figure 5). The AGC distribution is not highly related with the forest distribution in China, and the difference is mainly reflected in the northwest



and central south regions. For northwest region, although there are fewer forests, most of them are mature forests and over-mature forests with large volume per unit area, which is a cause of high carbon density. For central south region, there are more young forests and middle-aged forests in mountain areas, and the forests have gradually evolved into secondary forests. Secondary tree species dominate, resulting in sparse tree growth and low stand volume per unit area [47–49]. The northwest and southwest regions account for more than 70% of the country's AGB and AGC. The distribution of AGB and AGC is obviously different among regions, where the AGB and AGC in the northwest are 6.2 times and 6.3 times those in the north, respectively. Because of the differences in land area and forest coverage, the areas with high AGB density and AGC density are not necessarily the areas with high AGB and AGC. Ordinarily, the AGB and AGC density of each area can better reflect the actual situation of those areas. The average AGB density among the regions is  $91.34 \text{ Mg ha}^{-1}$ , the average AGC density is  $46.4 \text{ Mg ha}^{-1}$ , and they range from high to low in the following order: southwest, northwest, northeast, east, central south, and north, which is inconsistent with the order observed for AGB and AGC. For example, the AGB and AGC in east and southwest regions are lower than those in the south and north, but the AGB density and AGC density in the former two regions are relatively high. Compared with the national average AGB density and AGC density, the northwest and southwest regions have higher AGB and AGC density, as well as the highest AGB and AGC.

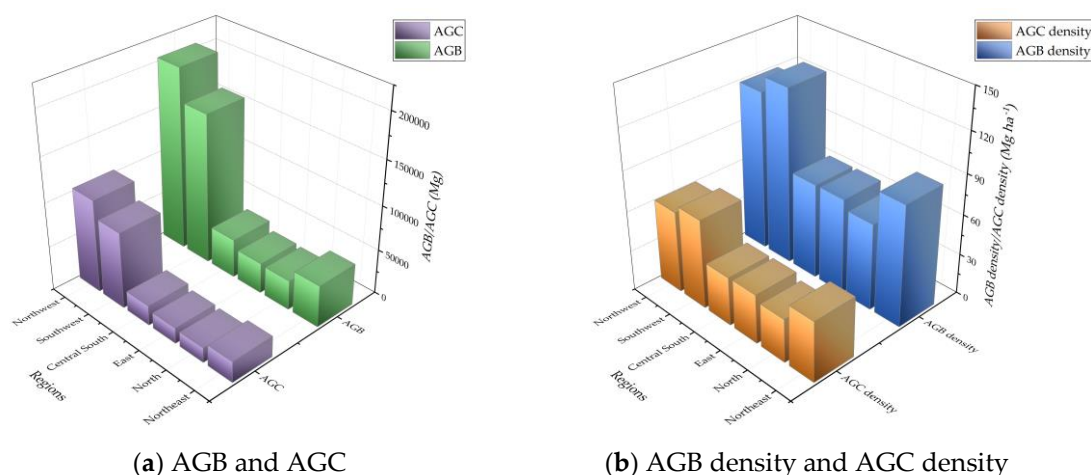


**Figure 5.** Comparative analysis of differences among regions. (a,b) represent the amount and density of aboveground biomass (AGB) and aboveground carbon (AGC), respectively, in the northwest, north, east, central south, southwest and northwest of China.

#### 4. Discussion

In recent years, application of the stand volume model has increased due to attention on AGB and AGC. Stand volume is an important variable for estimating AGB, AGC, and other factors of interest [50]. At present, the forest resources inventory in China is mainly based on field surveys, and the traditional method of obtaining the stand volume is to calculate the volume of each tree by using a unitary or binary volume table and then add up all trees in the sample plot. Obviously, such a method requires much manpower and many material resources. In addition, the traditional forest resources inventory takes a long time and takes place every five years, which is difficult to meet the current changing needs of forest management. In view of this, China urgently needs to build a high-precision forest volume estimation model to quickly and accurately estimate the stand volume and provide important decision-making basis for the forestry sector.

In this paper, stand density and forest basal area were introduced to calculate stand volume, and the average  $R^2$  for these factors among 37 forest types was 0.86 and 0.92, respectively. The results showed that volume can be better estimated by using the forest basal area-tree height model than by using the stand density-DBH-tree height model. Although the latter model meets the requirements,

its accuracy is not relatively high compared with that of other volume models [4,7,51,52]. One reason is that the model is based on sample plots at the national scale, at which the average DBH and tree height have greater errors than those measured at the scale of sample trees. The other reason is that current studies are mostly focused on pure forests, and we used the dominant species of sample plots as forest types, causing the growth rates of different species to have some influence on the accuracy of modeling. At the same scale, the model established in this paper can estimate the stand volume more accurately. We also used the traditional binary volume model to estimate stand volume, and the fitting results showed that the average  $R^2$  was 0.58 and varied significantly among forest types, indicating that it could be applied to some forest types well but not to others (Table A3). Validation precision was meanwhile performed but showed a low accuracy (Table A4). In the future, when calculating the stand volume of a certain site in China, forest factors could be obtained by remote sensing, unmanned aerial vehicles (UAVs), and three-dimensional laser scanning technology combined with a small number of field observations, after which the stand volume could be obtained quickly and conveniently by using the model given in this paper. Thus, the model developed here lays a good foundation for the accurate calculation of AGB and AGC.

Because the data set used in this research does not contain sample plot data from the forest resources inventory in China, it can represent the distribution but not total amount of AGB and AGC, while AGB density and AGC density can well represent the state of forest resources in China. The AGC density of Russia is  $40.4 \text{ Mg ha}^{-1}$  [8,53,54], that of the United States is  $58.8 \text{ Mg ha}^{-1}$  [55], that of Canada is  $30.7 \text{ Mg ha}^{-1}$  [56], and that of temperate zone is  $57.1 \text{ Mg ha}^{-1}$  [57], while the average AGC density of China estimated in this paper is  $48.15 \text{ Mg ha}^{-1}$ , which is far below the global average of  $86.00 \text{ Mg ha}^{-1}$ . Nevertheless, the AGC density of arbor forest in China has increased compared with that obtained in previous forest resource inventories [25,58,59]. This increase may be mainly due to the application of ecological civilization construction in China [60]. After the “Three North Shelterbelts” plan, China approved a new round of afforestation plan again. Through large-scale tree-planting activities (including artificial planting and aerial planting), the establishment of forest protection zones and the conversion of farmland to forestry land, China began afforestation throughout the country, implemented ecological projects, and comprehensively promoted the protection and management of the ecological environment. Over the past 40 years, the Ant Forest Project for voluntary tree planting has resulted in the accumulation of more than 55.52 million trees in desertification areas of China. The Three North Shelterbelt Project has resulted in 30.143 million hectares of afforestation, with the forest coverage increasing from 5.05% to 13.57%, and the reduction in soil erosion area reaching 61%. Furthermore, 1.944 billion mu of natural arbor forests has been restored, and 2.966 billion mu of natural forest has been effectively protected [20]. All these signs indicate that China’s AGC density will continue to increase.

The spatial pattern of AGC density in China is generally consistent with the spatial distribution of AGB density. There are obvious differences in topography, climate, river flow, and vegetation types between the northern and southern regions of China. Influenced by natural environment, people in different regions also display large differences in production mode, living habits, and cultural traditions. Based on the AGC density data for different regions in different survey periods, the AGC density in the north, southwest and northwest has been increasing gradually, with the most significant increase in the northwest: a net increase of  $34.52 \text{ Mg ha}^{-1}$  (Figure 6). The AGC density in the northeast first increased and then decreased, while that in the north and central south first decreased and then increased. The most significant decrease occurred in the central south: a net decrease of  $4.96 \text{ Mg ha}^{-1}$ . The average AGC density of forests in China is larger in the southwest, northwest, and northeast regions than in the other regions, which is the same as the result obtained using data from the sixth and seventh forest inventories [3,61]. These three areas are mostly located in the vertical natural zone of subtropical mountainous areas, and most of them are subalpine coniferous forests with *Cupressus funebris* Endl., *Populus* spp. and *Pinus yunnanensis* Franch. as dominant species. These areas belong to the top forest communities in the cold and warm climate of mountainous areas and have high AGB.

Because of the high population density, the forests in the central, central south, east, and north areas are greatly affected by human activities, and most of them are planted forests with low AGB.

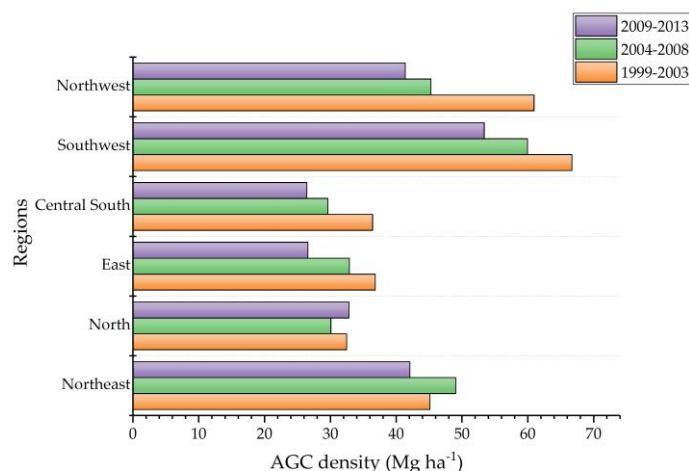


**Figure 6.** Aboveground carbon (AGC) density at three stages in different regions of China. The three periods correspond to the sixth, seventh, and eighth forest resources inventories.

Of course, in terms of practical deployment, this research also has certain limitations. Biomass includes aboveground biomass and underground biomass, and ecosystem carbon storage includes vegetation and soil. However, due to the scarcity of soil measurement data in China, only AGB and AGC has been studied in this paper. In addition, forest resources inventory data also contain other stand factors, such as stand age, tree species structure, and age group, which are closely related to AGB and AGC. However, this study did not consider the effect of these factors. In this case, we can perform more detailed research, for example, by carrying out analyses by age class (young forest, middle-aged forest, near-mature forest, mature forest, and over-mature forest), and aiming to use the multiperiod survey data to correctly assess of the source and sink functions of forests in China, in order to further evaluate the role of forests in global climate change.

## 5. Conclusions

This study proposed two models ( $M_1 = ad^bH^cN^f$ ,  $M_2 = aH^bG^c$ ) for calculating the stand volume of 37 forest types in China, and  $M_1$  was better than  $M_2$ . The precision and accuracy of the model met the standards. Compared with previous studies, the most significant contribution of this study is that it provides a low-cost, low-field workload, high-precision, large-scale model with which to calculate stand volume. Furthermore, we estimated AGB, AGB density, AGC, and AGC density by using the latest forest inventory data for China. The average AGC density of each forest type in China was much lower than the global level. Among the forest types, the AGC density of *Picea asperata* Mast., *Quercus* spp., and *Populus* spp. forest exhibited a relatively high AGC density. Among regions, southwest, northwest, and northeast had a relatively high AGC density. China needs to coordinate sustainable land management policies and the political framework of climate change, and adjust its economic development model to meet the common needs of economic development, energy conservation, and emission reduction.

Nevertheless, many questions remain, such as how to quickly obtain forest information by using new technologies. Further studies are recommended to increase the accuracy of the stock volume model and to use multi-period data to study the dynamics of biomass and carbon storage. In addition, shrub and herb biomass and carbon storage also have an important impact on the ecological environment. Therefore, the establishment of shrub and herb models will also be the focus of future research.

**Supplementary Materials:** The following are available online at <http://www.mdpi.com/1999-4907/10/8/650/s1>, Table S1: Sample plot database.

**Author Contributions:** Conceptualization, Z.F. and J.L.; Methodology, Z.F.; Validation, Z.F. and J.L.; Formal Analysis, J.L.; Investigation, Z.F. and J.L.; Resources, Z.F.; Data Curation, Z.F.; Writing—Original Draft Preparation, J.L.; Writing—Review & Editing, J.L. and Y.Z.; Visualization, J.L.; Supervision, Z.F.; Project Administration, Z.F.; Funding Acquisition, Z.F.

**Funding:** This research was jointly supported by the Fundamental Research Funds for the Central Universities (NO.2015ZCQ-LX-01) and the National Natural Science Foundation of China (No. U1710123).

**Acknowledgments:** We would like to acknowledge support from Beijing Key Laboratory for Precision Forestry, Beijing Forestry University, and to acknowledge all the people who have contributed to this paper.

**Conflicts of Interest:** The authors declare no conflict of interest.

## Appendix A

**Table A1.** Sampling designs for 31 provinces in China’s forest resources inventory.

Provinces	Sub-Pop.	Area (ha)	Grid (km)	Plot Shape	Plot Size (ha)
Beijing	/	16,410	2 × 2	Square	0.0667
Tianjin	/	11,305	2 × 2	Square	0.0667
Hebei	/	187,693	4 × 4	Square	0.06
Shanxi	/	156,623	4 × 4	Square	0.0667
InnerMongolia	/	11,830	8 × 8	Rectangular	0.06
Liaoning	/	145,739	4 × 8	Square	0.08
Jilin	/	189,193	4 × 16/3	Square	0.06
Heilongjiang	I	100,540	8 × 8	Square	0.06
	II	64,786	8 × 8	Rectangular	0.06
	III	289,282	4 × 8	Square	0.06
Shanghai	/	6341	2 × 1	Square	0.0667
Jiangsu	/	102,600	4 × 3	Square	0.0667
Zhejiang	/	101,800	4 × 6	Square	0.08
Anhui	/	138,165	4 × 3	Square	0.0667
Fujian	/	121,501	4 × 6	Square	0.0667
Jiangxi	/	166,946	8 × 8	Square	0.0667
Shandong	/	152,221	4 × 4	Square	0.0667
Henan	/	167,000	4 × 4	Square	0.08
Hubei	/	185,900	4 × 8	Square	0.0667
Hunan	/	211,835	4 × 8	Square	0.0667
Guangdong	/	176,769	6 × 8	Square	0.0667
Guangxi	/	237,600	6 × 8	Square	0.0667
Hainan	/	33,907	4 × 3	Square	0.0667
Chongqing	/	82,335	4 × 4	Square	0.0667
Sichuan	/	483,744	6 × 8	Square	0.0667
Guizhou	/	176,167	4 × 8	Square	0.0667
Yunnan	/	382,644	6 × 8	Square	0.0667
Xizang	/	1,228,436	6 × 8	Circular	0.0667
Shaanxi	/	205,977	4 × 8	Square	0.08
Gansu	I	449,734	2 × 3	Square	0.08
	II		3 × 3	Square	0.08
	III		4 × 8	Square	0.08
Qinghai	I	721,514	2 × 2	Square	0.08
	II		4 × 2	Square	0.08
Ningxia	/	51,955	2 × 2	Square	0.06
Xinjiang	I	164,700	3 × 4	Square	0.08
	II		6 × 4	Square	0.08

**Table A2.** Groups and common names corresponding to forest types (dominant species).

Group	Forest Type (Dominant Species)	Common Name
broad-leaved forest	<i>Abies fabri</i> (Mast.) Craib	Acacia rachii
	<i>Abrus</i> spp.	Birch
	<i>Betula</i> spp.	Ribbed Birch
	<i>Betula Costata</i> Trautv	White birch
	<i>Betula platyphylla</i> Suk.	Eucalyptus
	<i>Cryptomeria fortunei</i> Hooibrenk ex Otto et Dietr.	Larch
	<i>Cunninghamia lanceolata</i> (Lamb.) Hook.	Camphorwood
	<i>Cupressus funebris</i> Endl.	Other hard-and-broad trees
	<i>Eucalyptus robusta</i> Smith	Other soft-and-broad trees
	<i>Keteleeria fortunei</i> (Murr.) Carr.	Phoebe
	<i>Larix gmelinii</i> (Ruprecht) Kuzeneva	Quercus
	<i>Cinnamomum camphora</i> (L.) Presl.	Locust
	Other hard-and-broad trees	Willow
	Other pine trees	Schima
	Other soft-and-broad trees	Linden
	<i>Phoebe zhenman</i> S. Lee et F. N. Wei	Elm
coniferous forest	<i>Picea asperata</i> Mast.	Fir
	<i>Pinus armandii</i> Franch.	Japanese cedar
	<i>Pinus densata</i> Mast.	China fir
	<i>Pinus densiflora</i> Sieb. et Zucc.	Weeping cypress
	<i>Pinus elliotii</i> Engelman	Keteleeria
	<i>Pinus kesiya</i> Royle ex Gordon var. <i>langbianensis</i> (A.Chev) Gaussen	Other pine trees
	<i>Pinus koraiensis</i> Siebold et Zuccarini	Spruce
	<i>Pinus massoniana</i> Lamb.	Pinus armandi
	<i>Pinus sylvestris</i> Linn. var. <i>mongolica</i> Litv.	Alpine pine
	<i>Pinus tabulaeformis</i> Carr.	Japanese red pine
	<i>Pinus taiwanensis</i> Hayata	Sash pine
	<i>Pinus thunbergii</i> Parlatore	Simao pine
	<i>Pinus yunnanensis</i> Franch.	Korean pine
	<i>Populus</i> spp.	Masson pine
	<i>Quercus</i> spp.	Mongolian scotch pine
	<i>Robinia pseudoacacia</i> Linn.	Chinese pine
	<i>Salix</i> spp.	Huangshan Pine
	<i>Schima superba</i> Gardn. et Champ.	Lodgepole pine
	<i>Tilia tuan</i> Szyszyl.	Yunnan pine
	<i>Tsuga chinensis</i> (Franch.) Pritz.	Poplar
	<i>Ulmus pumila</i> Linn.	Hemlock

Table A3. Fitting results for binary volume model.

Forest Type	n	$M_0 = ad^b H^c$						$R^2$
		a	SE(a)	b	SE(b)	c	SE(c)	
<i>Abies fabri</i> (Mast.) Craib	72	3.784	3.031	1.349	0.296	0.144	0.215	0.37
<i>Abrus</i> spp.	8	0.325	0.462	0.266	0.459	2.054	0.472	0.90
<i>Betula</i> spp.	98	1.713	0.620	1.099	0.140	0.285	0.210	0.54
<i>Betula Costata</i> Trautv	14	1.209	1.249	1.393	0.541	0.000	0.861	0.78
<i>Betula platyphylla</i> Suk.	206	2.732	0.813	0.064	0.091	1.167	0.127	0.37
<i>Cryptomeria fortunei</i> Hooibrenk ex Otto et Dietr.	9	8.884	8.498	0.991	0.293	0.097	0.114	0.63
<i>Cunninghamia lanceolata</i> (Lamb.) Hook.	318	2.369	0.642	1.204	0.120	0.303	0.077	0.38
<i>Cupressus funebris</i> Endl.	219	0.613	0.155	1.027	0.091	0.895	0.103	0.62
<i>Eucalyptus robusta</i> Smith	90	1.850	0.985	0.442	0.315	0.984	0.239	0.39
<i>Keteleeria fortunei</i> (Murr.) Carr.	182	21.074	30.222	0.533	0.766	0.000	0.993	0.15
<i>Larix gmelinii</i> (Ruprecht) Kuzeneva	294	2.637	0.663	0.581	0.093	0.697	0.107	0.39
<i>Cinnamomum camphora</i> (L.) Presl.	4	0.376	0.962	0.000	1.239	1.950	1.110	0.96
Other hard-and-broad trees	134	0.162	0.069	1.693	0.101	0.543	0.202	0.65
Other pine trees	8	0.085	0.077	2.046	0.347	0.523	0.229	0.79
Other soft-and-broad trees	87	1.824	0.570	0.635	0.093	0.795	0.159	0.60
<i>Phoebe zhennan</i> S. Lee et F. N. Wei	6	0.022	0.181	2.383	2.306	0.786	1.051	0.64
<i>Picea asperata</i> Mast.	479	5.013	0.879	1.078	0.089	0.230	0.077	0.52
<i>Pinus armandii</i> Franch.	29	6.742	5.018	1.007	0.385	0.000	0.343	0.34
<i>Pinus densata</i> Mast.	64	2.372	0.956	0.000	0.268	1.633	0.253	0.83
<i>Pinus densiflora</i> Sieb. et Zucc.	11	0.546	0.579	1.457	0.303	0.457	0.487	0.83
<i>Pinus elliotii</i> Engelmann	22	2.364	3.068	1.157	0.557	0.022	0.174	0.25
<i>Pinus kesiya</i> Royle ex Gordon var. <i>langbianensis</i> (A.Chev) Gaussen	28	87.330	50.705	0.150	0.278	0.002	0.273	0.02
<i>Pinus koraiensis</i> Siebold et Zuccarini	8	5.134	7.262	1.167	0.821	0.000	0.417	0.60
<i>Pinus massoniana</i> Lamb.	336	4.353	0.936	0.980	0.103	0.180	0.104	0.37
<i>Pinus sylvestris</i> Linn. var. <i>mongolica</i> Litv.	14	1.576	1.325	1.593	0.368	0.000	0.329	0.70
<i>Pinus tabulaeformis</i> Carr.	11	3.047	0.797	1.383	0.131	0.000	0.137	0.55
<i>Pinus taiwanensis</i> Hayata	4	2.709	2.253	1.585	1.618	0.023	1.218	0.95
<i>Pinus thunbergii</i> Parlatore	14	0.258	0.433	0.067	0.571	2.085	0.907	0.53
<i>Pinus yunnanensis</i> Franch.	184	2.120	0.444	1.677	0.144	0.000	0.151	0.80
<i>Populus</i> spp.	296	3.329	0.805	1.094	0.128	0.214	0.078	0.50
<i>Quercus</i> spp.	578	2.168	0.379	0.535	0.077	0.931	0.095	0.44
<i>Robinia pseudoacacia</i> Linn.	39	0.584	0.471	0.527	0.265	1.319	0.443	0.45
<i>Salix</i> spp.	36	0.695	0.594	0.223	0.318	1.496	0.300	0.56
<i>Schima superba</i> Gardn. et Champ.	16	1.369	1.174	0.231	0.426	1.382	0.332	0.76
<i>Tilia tuan</i> Szyszyl.	18	0.042	0.064	0.470	0.773	2.421	0.692	0.68
<i>Tsuga chinensis</i> (Franch.) Pritz.	6	0.085	0.127	0.948	0.965	1.486	0.963	0.94
<i>Ulmus pumila</i> Linn.	27	0.328	0.350	0.370	0.338	1.602	0.400	0.53



**Table A4.** Validation of the stand volume precision binary volume model of different forest types.

Forest Type	$M_0 = ad^b H^c$					
	<i>n</i>	BIAS	BIAS%	RMSE	RMSE%	$R^2_{emp}$
<i>Abies fabri</i> (Mast.) Craib	18	−116.878	−41.444	145.310	51.526	0.35
<i>Abrus</i> spp.	2	−35.023	−16.856	93.724	45.108	0.57
<i>Betula</i> spp.	25	12.710	4.148	147.679	48.198	0.73
<i>Betula Costata</i> Trautv	3	−7.225	−10.302	12.595	17.959	0.21
<i>Betula platyphylla</i> Suk.	51	−22.239	−20.507	75.932	70.019	0.38
<i>Cryptomeria fortunei</i> Hooibrenk ex Otto et Dietr.	2	−33.926	−60.551	53.802	96.025	0.49
<i>Cunninghamia lanceolata</i> (Lamb.) Hook.	79	−29.391	−27.698	62.854	59.235	0.12
<i>Cupressus funebris</i> Endl.	55	−12.185	−69.888	15.966	91.571	0.28
<i>Eucalyptus robusta</i> Smith	22	27.124	57.325	41.120	86.905	0.24
<i>Keteleeria fortunei</i> (Murr.) Carr.	48	−8.513	−13.906	37.974	62.032	0.36
<i>Larix gmelinii</i> (Ruprecht) Kuzeneva	73	−22.215	−43.409	30.424	59.451	0.51
<i>Cinnamomum camphora</i> (L.) Presl.	1	−16.691	−24.677	42.299	62.536	0.09
Other hard-and-broad trees	33	4.794	3.371	54.828	38.558	0.80
Other pine trees	2	−29.521	−23.042	48.311	37.709	0.04
Other soft-and-broad trees	22	1.103	0.425	50.061	19.268	0.82
<i>Phoebe zhennan</i> S. Lee et F. N. Wei	1	−0.276	−0.635	22.014	50.767	0.25
<i>Picea asperata</i> Mast.	120	−31.003	−30.775	76.481	75.920	0.15
<i>Pinus armandii</i> Franch.	7	−35.244	−52.462	81.124	120.756	0.29
<i>Pinus densata</i> Mast.	16	−44.018	−46.639	72.459	76.775	0.02
<i>Pinus densiflora</i> Sieb. et Zucc.	3	25.862	14.776	95.619	54.632	0.14
<i>Pinus elliotii</i> Engelmann	5	4.409	6.685	40.048	60.713	0.60
<i>Pinus kesiya</i> Royle ex Gordon var. <i>langbianensis</i> (A.Chev) Gaussen	7	11.064	11.301	51.230	52.327	0.25
<i>Pinus koraiensis</i> Siebold et Zuccarini	2	0.451	0.742	35.625	58.643	0.54
<i>Pinus massoniana</i> Lamb.	84	−0.023	−0.037	27.088	44.496	0.37
<i>Pinus sylvestris</i> Linn. var. <i>mongolica</i> Litv.	3	0.644	1.087	31.786	53.683	0.78
<i>Pinus tabulaeformis</i> Carr.	3	8.622	10.943	84.007	106.619	0.22
<i>Pinus taiwanensis</i> Hayata	1	2.739	0.980	149.686	53.568	0.56
<i>Pinus thunbergii</i> Parlato	3	8.930	21.105	20.827	49.222	0.64
<i>Pinus yunnanensis</i> Franch.	44	−9.961	−68.416	12.052	82.781	0.76
<i>Populus</i> spp.	74	−0.636	−1.653	15.097	39.261	0.73
<i>Quercus</i> spp.	144	8.981	19.871	30.568	67.632	0.42
<i>Robinia pseudoacacia</i> Linn.	10	5.616	6.835	33.256	40.473	0.64
<i>Salix</i> spp.	9	−5.621	−7.254	39.167	50.541	0.51
<i>Schima superba</i> Gardn. et Champ.	4	8.462	8.489	50.323	50.485	0.68
<i>Tilia tuan</i> Szyszyl.	4	−1.861	−3.098	36.284	60.408	0.36
<i>Tsuga chinensis</i> (Franch.) Pritz.	2	−10.277	−15.895	31.432	48.614	0.71
<i>Ulmus pumila</i> Linn.	7	−5.441	−8.807	23.782	38.495	0.38

## References

1. Yang, X.; Wu, B.; Zhang, J.; Lin, D.; Chang, S. Progress of research into carbon fixation and storage of forest ecosystems. *J. Beijing Norm. Univ.* **2005**, *41*, 172–177.
2. Liu, H.; Lei, R. Research Methods and Advances of AGC and Balance in Forest Ecosystems of China. *Acta Bot. Boreali-Occident. Sin.* **2005**, *25*, 835–843.
3. Li, H.; Lei, Y.; Zeng, W. Forest AGC in China Estimated Using Forestry Inventory Data. *Sci. Silvae Sin.* **2011**, *47*, 7–12.
4. Kang, L.; Meng, W.; He, H. Comparative study on stand volume models—Taking middle-aged Chinese fir in Hunan Province State-owned Forest Farm as an example. *Trop. For.* **2018**, *46*, 14–18.
5. Zhang, N.; Feng, Z.; Feng, Y.; Fan, J. Research on coniferous forest volume estimation model for Wangyedian experimental forest farm. *J. Cent. South Univ. For. Technol.* **2013**, *33*, 83–87.
6. Liu, F. Study on the Growth Dynamic Forecast Model of Chinese fir Stand in Fujian Province. *For. Prospect Des.* **2018**, *38*, 1–4.
7. Zeng, W.; Yang, X.; Chen, X. Comparison on Prediction Precision of One-variable and Two-variable Volume Model on Tree-level and Stand-level. *Cent. South For. Inventory Plan.* **2017**, *36*, 1–6.
8. Zhou, S. Construction of Precision Analysis Model for Binary Volume and Volume of Forest Trees. *Technol. Innov. Appl.* **2015**, *34*, 16–17.
9. Reis, A.A.D.; Carvalho, M.C.; Mello, J.M.D.; Gomide, L.R.; Filho, A.C.F.; Junior, F.W.A. Spatial prediction of basal area and volume in Eucalyptus stands using Landsat TM data: An assessment of prediction methods. *N. Z. J. For. Sci.* **2018**, *48*, 1. [[CrossRef](#)]
10. Zhang, X. *Study on the Impact of Terrain on Community Distribution Pattern in Natural Secondary Forest*; Northeast Forestry University: Jilin, China, 2007.
11. Tong, J.; Jin, G.; Li, F.; Jia, W.; Cui, X. AGC density and distribution in soft broad-leaved mixed forest of different age classes in Heilongjiang Province, Northeast China. *Chin. J. Ecol.* **2014**, *33*, 3191–3202.
12. Wang, X.; Qi, G.; Yu, D.; Zhou, L.; Dai, L. AGC, density, and distribution in forest ecosystems in Jilin Province of Northeast China. *Chin. J. Appl. Ecol.* **2011**, *22*, 2013–2020.
13. Wang, W.; Song, L.; Sui, X. Estimation of Forest AGB and Its Temporal and Spatial Distribution Patterns in Maershan Forest Farm. *J. Northeast For. Univ.* **2010**, *38*, 47–49.
14. Guo, C.; Zhou, Z.; Kang, F.; Sun, J. The alteration of carbon stock of forest ecosystem by tree species composition in Taiyue Mountain. *Chin. J. Ecol.* **2014**, *33*, 2012–2018.
15. Kauppi, P.E.; Mielikä Inen, K.; Kuusela, K. AGB and carbon budget of European forests, 1971 to 1990. *Science* **1992**, *256*, 70–74. [[CrossRef](#)] [[PubMed](#)]
16. Liu, G.; Fu, G.; Fang, J. Carbon dynamics of Chinese forests and its contribution to global carbon balance. *Acta Ecol. Sin.* **2000**, *5*, 733–740.
17. West, P.W. *Tree and Forest Measurement*; Springer: Berlin/Heidelberg, Germany, 2005.
18. Di Cosmo, L.; Gasparini, P.; Tabacchi, G. A national-scale, stand-level model to predict total above-ground tree AGB from growing stock volume. *For. Ecol. Manag.* **2016**, *361*, 269–276. [[CrossRef](#)]
19. Fang, J.; Chen, A.; Peng, C.; Zhao, S.; Ci, L. Changes in forest AGB AGC in China between 1949 and 1998. *Science* **2001**, *292*, 2320–2322. [[CrossRef](#)]
20. Qiu, Z. *Measurement and Statistics of Land-Surface Forest Vegetation Carbon Sink in China*. Ph.D. Thesis, Beijing Forestry University, Beijing, China, 2019.
21. Wang, X.; Feng, Z.; Ou, Z. Vegetation AGC and density of forest ecosystems in China. *Chin. J. Appl. Ecol.* **2001**, *1*, 13–16.
22. Zhao, M.; Zhou, G. AGC of Forest Vegetation and Its Relationship with Climatic Factors. *Sci. Geogr. Sin.* **2004**, *1*, 50–54.
23. Somogyi, Z.; Cienciala, E.; Mäkipää, R.; Muukkonen, P.; Lehtonen, A.; Weiss, P. Indirect methods of large-scale forest AGB estimation. *Eur. J. For. Res.* **2007**, *126*, 197–207. [[CrossRef](#)]
24. Zhou, G.; Wang, Y.; Jiang, Y.; Yang, Z. Estimating AGB and net primary production from forest inventory data: A case study of China's Larix forests. *For. Ecol. Manag.* **2002**, *169*, 149–157. [[CrossRef](#)]
25. Fang, J.Y.; Wang, G.G.; Liu, G.H.; Xu, S.L. Forest AGB of China: An estimate based on the AGB–volume relationship. *Ecol. Appl.* **1998**, *8*, 1084–1091.

26. Johnson, W.C.; Sharpe, D.M. The ratio of total to merchantable forest AGB and its application. *Revue Can. Rech. For.* **1983**, *13*, 372–383. [[CrossRef](#)]
27. Liu, J.; Feng, Z.; Mannan, A.; Khan, T.; Cheng, Z. Comparing Non-Destructive Methods to Estimate Volume of Three Tree Taxa in Beijing, China. *Forests* **2019**, *10*, 92. [[CrossRef](#)]
28. Fang, J.; Liu, G.; Zhu, B.; Wang, X.; Liu, S. Carbon Cycle of Three Temperate Forest Ecosystems in Dongling Mountain, Beijing. *Sci. Sin.* **2006**, *36*, 533–543.
29. Huang, X.; Dai, D.; Huang, C.; Teng, M.; Zhou, Z. Researches Progress in AGB and Productivity of *Pinus massoniana*. *World For. Res.* **2019**, *32*, 53–58.
30. Guo-Qing, W.; Xue-Feng, C. Studies on stand dynamic growth model for larch in Jilin in China. *J. For. Res.* **2004**, *15*, 323–326. [[CrossRef](#)]
31. Shao, W.; Cai, J.; Wu, H.; Liu, J. An Assessment of AGC in China's Arboreal Forests. *Forests* **2017**, *8*, 110. [[CrossRef](#)]
32. LY/T 2188.1-2013, Forest resource data collection technical specification—Part 1: Forest continuous inventory. In Industry Standard—Forestry.
33. Knowe, S.A.; Foster, G.S. Application of Growth Models for Simulating Genetic Gain of Loblolly Pine. *For. Sci.* **1989**, *35*, 211–228.
34. Rehfeldt, G.E.; Wykoff, W.R.; Hoff, R.J.; Steinhoff, R.J. Genetic Gains in Growth and Simulated Yield of *Pinus monticola*. *For. Sci.* **1991**, *37*, 326–342.
35. Buford, M.A.; Burkhart, H.E. Genetic Improvement Effects on Growth and Yield of Loblolly Pine Plantations. *For. Sci.* **1987**, *33*, 707–724.
36. Nance, W.L.; Bay, C.F. Incorporating Genetic Information in Growth and Yield Models. In Proceedings of the 15th Southern Forest Tree Improvement Conference, Starkville, MS, USA, 19–21 June 1979.
37. Wang, N.; Yang, Y.; Dai, W. The Basal Area Growth Model of Larch Plantation Based on Richards Equation. *For. Eng.* **2015**, *31*, 22–25.
38. Zhang, L.; Hui, G.; Sun, C. Comparison of different stand density measures. *J. For. Environ.* **2011**, *31*, 257–261.
39. Qin, Z.; Dong, W.; Liu, T.; Zhang, Y.; Guo, J.; Wu, Y. Responses of understory plant diversity to stand density in natural secondary forests of *Pinus tabulaeformis*. *J. Shanxi Agric. Univ. (Nat. Sci. Edit.)* **2019**, *39*, 61–67.
40. LY/T 1353-1999, Standing Volume Table. In Industry Standard-Forestry.
41. Maas, D.; Hox, J. The influence of violations of assumptions on multilevel parameter estimates and their standard errors. *Comput. Stat. Data Anal.* **2003**, *46*, 427–440. [[CrossRef](#)]
42. Zhang, H.; Feng, Z.; Chen, P.; Chen, X. Development of a Tree Growth Difference Equation and Its Application in Forecasting the AGB Carbon Stocks of Chinese Forests in 2050. *Forests* **2019**, *10*, 582. [[CrossRef](#)]
43. Friedlingstein, P.; Cox, P.; Betts, R.; Bopp, L.; Bloh, W.V.; Brovkin, V.; Cadule, P.; Doney, S.; Eby, M.; Fung, I. Climate-Carbon Cycle Feedback Analysis: Results from the C4MIP Model Intercomparison. *J. Clim.* **2006**, *19*, 3337–3353. [[CrossRef](#)]
44. Landman, W. Climate change 2007: The physical science basis. *S. Afri. Geogr. J.* **2007**, *92*, 86–87. [[CrossRef](#)]
45. Dixon, R.K.; Solomon, A.M.; Brown, S.; Houghton, R.A.; Trexler, M.C.; Wisniewski, J. Carbon pools and flux of global forest ecosystems. *Science* **1994**, *263*, 185–190. [[CrossRef](#)]
46. Huang, C.; Zhang, J.; Yang, W.; Tang, X.; Zhao, A. Dynamics on forest carbon stock in Sichuan Province and Chongqing City. *Acta Ecol. Sin.* **2008**, *28*, 966–975.
47. Li, F.; Li, M.; Shi, Z. Estimates Stand Age Distribution Based on Forest Survey and Remote Sensing data. *For. Eng.* **2018**, *34*, 30–34.
48. Zhao, M.; Yue, T.; Zhao, N. Spatial distribution of forest vegetation carbon stock in China based on HASM. *Acta Geogr. Sin.* **2013**, *68*, 1212–1224.
49. Chen, X. *Study on the Influencing Factors of Regional Forest Resources Change in China*; Beijing Forestry University: Beijing, China, 2007.
50. Saud, P.; Lynch, T.B.; KC, A.; Guldin, J.M. Using quadratic mean diameter and relative spacing index to enhance height–diameter and crown ratio models fitted to longitudinal data. *Forestry* **2016**, *89*, 215–229. [[CrossRef](#)]
51. Sisay, K.; Thurnher, C.; Belay, B.; Lindner, G.; Hasenauer, H. Volume and Carbon Estimates for the Forest Area of the Amhara Region in Northwestern Ethiopia. *Forests* **2017**, *8*, 122. [[CrossRef](#)]
52. Zhang, X.; Zhang, J.; Duan, A. Compatibility of Stand Volume Model for Chinese Fir Based on Tree-Level and Stand-Level. *Sci. Silvae Sin.* **2014**, *50*, 82–87.

53. Alexeyev, V.; Birdsey, R.; Stakanov, V.; Korotkov, I. Carbon in vegetation of Russian forests: Methods to estimate storage and geographical distribution. *Water Air Soil Pollut.* **1995**, *82*, 271–282. [[CrossRef](#)]
54. Isaev, A.; Korovin, G.; Zamolodchikov, D.; Utkin, A.; Pryaznikov, A. Carbon Stock and Deposition in Phytomass of the Russian Forests. *Water Air Soil Pollut.* **1995**, *82*, 247–256. [[CrossRef](#)]
55. Murillo, J.C.R. Temporal Variations in the Carbon Budget of Forest Ecosystems in Spain. *Ecol. Appl.* **1997**, *7*, 461–469. [[CrossRef](#)]
56. Harmon, M.E. AGC and Sequestration in the Russian Forest Sector. *Ambio* **1996**, *25*, 284–288.
57. Kurz, W.A.; Apps, M.J.; Webb, T.M.; Mcnamee, P.J. The carbon budget of the Canadian forest sector: Phase I. *Simulation* **1993**, *61*, 139–144. [[CrossRef](#)]
58. Heath, L.S.; Kauppi, P.E.; Burschel, P.; Gregor, H.D.; Guderian, R.; Kohlmaier, G.H.; Lorenz, S.; Overdieck, D.; Scholz, F.; Thomasius, H. Contribution of temperate forests to the world's carbon budget. *Water Air Soil Pollut.* **1993**, *70*, 55–69. [[CrossRef](#)]
59. Lin, Q.; Hong, W. Summary of Research on Forest AGC in China. *Chin. Agric. Sci. Bull.* **2009**, *25*, 220–224.
60. Xu, X.; Cao, M.; Li, K. Temporal-Spatial Dynamics of AGC of Forest Vegetation in China. *Prog. Geogr.* **2007**, *6*, 1–10.
61. Bai, Y.; Huang, Y.; Wang, M.; Huang, S.; Sha, C.; Ruan, J. The progress of ecological civilization construction and its indicator system in China. *Acta Ecol. Sin.* **2011**, *31*, 6295–6304.



© 2019 by the authors. Licensee MDPI, Basel, Switzerland. This article is an open access article distributed under the terms and conditions of the Creative Commons Attribution (CC BY) license (<http://creativecommons.org/licenses/by/4.0/>).